# Strain tunable light transmission through a 90° bend waveguide in a two-dimensional photonic crystal

**ARTICLE** *in* APPLIED PHYSICS LETTERS · SEPTEMBER 2003

Impact Factor: 3.3 · DOI: 10.1063/1.1604467 · Source: IEEE Xplore



**3 AUTHORS**, INCLUDING:

N. Malkova
KLA-Tencor
**65** PUBLICATIONS **456** CITATIONS

SEE PROFILE

# Strain tunable light transmission through a 90° bend waveguide in a two-dimensional photonic crystal

Natalia Malkova, Sungwon Kim, and Venkatraman Gopalan[a)]
*Materials Research Institute, Pennsylvania State University, University Park, Pennsylvania 16802*

(Received 21 April 2003; accepted 27 June 2003)

We report a device based on strain-tunable light propagation through a 90° bend waveguide based on a two-dimensional photonic crystal. This is achieved by the splitting of a doubly degenerate defect state, by means of a symmetrical distortion of the lattice, locally near the bend. The resonant coupling of the photon modes between the two waveguide arms across the bend can be tuned by the symmetry and the magnitude of the local distortion of the lattice. © *2003 American Institute of Physics.* [DOI: 10.1063/1.1604467]

Tunability of the properties of photonic crystals is key to technological applications. Guiding and bending of the electromagnetic waves through highly localized defect modes in a photonic crystal has been reported.[1] The most important feature of these coupled cavity waveguides is the possibility of constructing lossless and reflectionless bends.[2] This ability has a crucial role in overcoming the problem of guiding light around sharp corners in optical circuits.[3] A recent study[4] reports tunable light propagation in Y-shaped waveguides based on two-dimensional photonic crystals with a hexagonal lattice using liquid crystals as linear defects. In this letter, we propose to use a tunable splitting of the degeneracy of a defect state for increasing the defect mode coupling at the corner of a coupled cavity 90° bend waveguide. An analogy may be drawn to the Jahn–Teller effect in solids,[5] which involves the splitting of degenerate electronic states by a suitable distortion of the lattice.

As a model crystal, we consider a square photonic crystal of the dielectric rods with a lattice constant $a$, rod radius, $r=0.2a$ and the dielectric constant $\epsilon_r=11.9$, embedded in an air matrix. Only modes with odd (TM-like) symmetry are considered, since that is the symmetry of the bands exhibiting a gap for the square lattice. We study the system shown in the inset of Fig. 1. Waveguided modes by the defect rods shown, with radius $r_d=0.3a$ and the same dielectric constant $\epsilon_d=11.9$ as the other rods, will be investigated. We are interested in double degenerate state $E$, giving the defect level inside the first band gap, and represented by the two $1\times2$ column basis vectors having the shape of the $|p_x\rangle$ and $|p_y\rangle$ orbitals.[6] This is the specific state under our consideration, for two reasons. First, we want to use the splitting of the double degenerate state for tuning the light propagation. Second, in the case of the coupled cavities, this state, being described by the $|p_x\rangle$ and $|p_y\rangle$ orbitals, gives a good coupling for light propagation along the $x$ axis and the $y$ axis, respectively.

To analyze this system, we use the finite difference time domain (FDTD) technique described in Ref. 7. Our computational domain is shown in the inset of Fig. 1. It contained $17\times15$ unit cells. Each unit cell was divided into $20\times20$ discretization grid cells. The computational domain was surrounded by perfect matched layers, with the thickness corresponding to ten layers of the discretization grid. The total number of the time steps was 100 000, with each time step $\Delta t=\Delta x/(2c)$. The source was simulated as a Gaussian beam in time domain and in the coordinate space with the width of the beam equal to 40 grid cells. To analyze the transmission of the structure, we collected the signal at the output of the waveguide structure and compared this data with the reference signal collected at the input of the structure, as described in Ref. 8. The computed transmission coefficient of the initial structure is shown by dashed line in Fig. 1.

We denote the input waveguide branch (before bending) as the $x$ arm, and the output branch (after bending) as the $y$ arm. When studying this structure, we note that each of the two waveguide arms of the coupled cavity defect crystal studied is characterized by two defect bands, with $p_x$ and $p_y$ symmetries.[6] From the supercell calculations we conclude

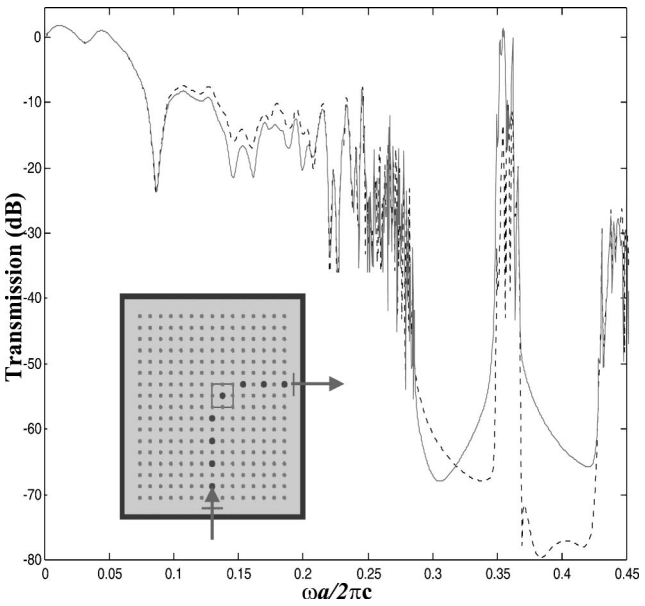


FIG. 1. Computed transmission coefficient of the structure with $\Delta r/a=0$ (dashed line) and 0.15 (solid line). Inset presents the calculation domain of the waveguide structure studied. Perfect matching layer boundaries, the source, and the corner cell are shown.

[a)]Electronic mail: vgopalan@psu.edu

 

that, in the infinite one defect line structure, the lower energy band ($\omega_{\|}\sim 0.354$) in each case is characterized by the symmetry of the $p$ orbital directed along the defect chain, that is $p_x$ for the $x$ arm and $p_y$ for the $y$ arm. The higher energy band ($\omega_{\perp}\sim 0.360$) in each case is characterized by the orthogonal states, i.e., the $p_y$ orbitals for the $x$ arm and $p_x$ orbitals for the $y$ arm. It is intuitive that the strongest coupling of the cavity modes (and therefore, the highest transmission) will be in the case when the light propagates through the $p_x$ band before the bend and through the $p_y$ band after bending. However, since the distance between the two bands is small, the light can tunnel at the corner from a $p_x$ to a $p_x$ orbital state. But in such a case, a lot of energy is lost due tunneling as well as due to a poor coupling between the $p_x$ modes in the $y$ arm after bending. As a result, the transmission of such a structure will be small (dashed line in Fig. 1).

Now let us consider the corner cell, shown in the inset of Fig. 1. Our problem is to find a perturbation $V$ of the distortions of the lattice, which results in such a splitting of the double degenerate $E$ state, that will result in maximum coupling between the guided modes of the two branches. The solution can be found from the eigenvalue problem $[H_0(\mathbf{r})+V(\mathbf{r})]\Psi(\mathbf{r})=E\Psi(\mathbf{r})$ for the eigenfunction $\Psi(\mathbf{r})=\Sigma_{i=x,y}A_i p_i(\mathbf{r})$, where the solution for the nonperturbed Hamiltonian $H_0|p_i\rangle=E|p_i\rangle$ gives the double degenerate state with the eigenvalue $E=\omega_0$. In the first approximation, with respect to magnitude of the lattice distortion, the perturbation can be extended over normal symmetrized displacements $V(\mathbf{r})=\Sigma_{\alpha}\mathbf{R}_{\alpha}\cdot\partial V^{\alpha}/\partial\mathbf{r}|_0$, where the deformation potential $\partial V^{\alpha}/\partial r$ is calculated at the zero lattice distortion.[9] In the case of the square lattice, there are allowed $2A_1$, $B_1$, $2B_2$, and $2E$ normal irreducible distortions. The $A_1$ perturbation is the total symmetrical one, while $B_{1,2}$ and $E$ are antisymmetrical.[9]

As follows from the Jahn–Teller theorem,[9] to split the doubly degenerate $E$ photonic state the matrix element of the corresponding perturbation, $V_{ij}^{\alpha}=\int p_i(\mathbf{r})V^{\alpha}(\mathbf{r})p_j(\mathbf{r})d\mathbf{r}\neq 0$. From the symmetry analysis, this matrix element is nonzero only for the $A_1$, $B_1$, and $B_2$ perturbations. Since for the total symmetrical distortion $A_1$, $V_{xx}^{A_1}=V_{yy}^{A_1}$ and $V_{xy}^{A_1}=0$, the interaction of the photonic $E$ state with the $A_1$ perturbation results in equal shifts of each of the double degenerate states without lifting the degeneracy. For the antisymmetrical $B_{1,2}$ distortions, $V_{xx}^{B_1}=-V_{yy}^{B_1}$, $V_{xy}^{B_1}=0$, while $V_{xx}^{B_2}=V_{yy}^{B_2}=0$, $V_{xy}^{B_2}=V_{xy}^{B_2}$. As a result, the degeneracy of the $E$-photonic mode is removed, resulting in two levels $\omega_{1,2}^{B1}=\omega_0\pm V_{xx}^{B_1}$ and $\omega_{1,2}^{B2}=\omega_0\pm V_{xy}^{B_2}$, being described by the $|p_x\rangle$ and $|p_y\rangle$ orbitals for the $B_1$ distortion and by $|p_x\pm p_y\rangle$ orbitals for the $B_2$ distortion.

We present supercell plane wave calculations and FDTD simulations of the two-dimensional one-defect crystal. For the supercell plane wave calculation, we followed the usual technique,[10] working with supercell including 16 rods. Figure 2 shows the dependence of the frequency splitting of the defect mode on the relative amplitude of the distortion for the $B_1$ and $B_2$ perturbations. The data obtained by the supercell plane wave technique (dashed lines) and by the FDTD calculations (solid lines) are in reasonable agreement. The

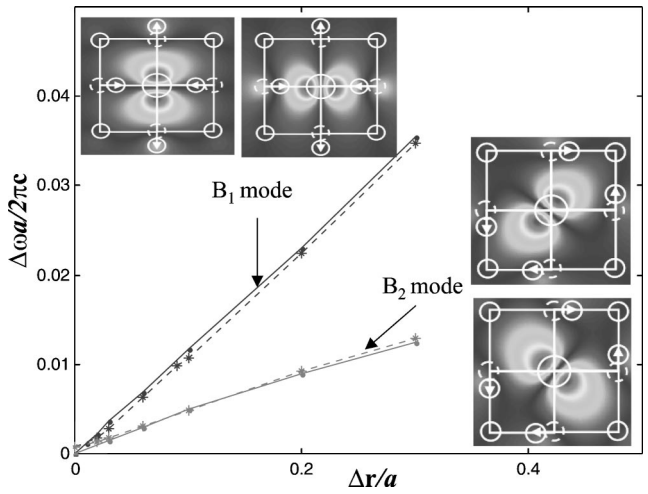


FIG. 2. Dependence of the frequency splitting of the double degenerate defect state on the relative amplitude of the distortion for the case of the $B_{1,2}$ perturbations. The data obtained from the supercell plane wave and FDTD calculations are shown by dashed and solid lines, respectively. Insets show the distribution of the electric field intensity for the split states. The Jahn–Teller cell with the corresponding displacements of the nearest neighbors to the central defect is overlaid.

magnitude of the splitting of the defect level shows a fairly linear scaling with the amplitude of the distortion for both of the perturbations, which validates the linear approximation of the perturbative potential for small distortions of the lattice. The data for the electric field distribution (see inset in Fig. 2), supports the theoretical prediction that the split states are characterized by the $|p_x\rangle$ and $|p_y\rangle$ orbitals in the case of the $B_1$ perturbation, and by the $|p_x\pm p_y\rangle$ orbitals in the case of the $B_2$ perturbation.

From the analysis follows that in the case of the waveguide structure studied, we have to distort the corner cell by means of the $B_2$ perturbation in order to get the strongest coupling between the guiding modes of the two branches. We present in Fig. 3 the relative transmission intensity inside the band gap for the structure with the distortion of the corner cell (see inset) $\Delta r/a=0$, 0.05, 0.15, and 0.3. We observe an increase in the transmission of light when $\Delta r>0$. The effect shows resonant behavior with the maximum at $\Delta r/a=0.15$ (Fig. 3 star markers). Figures 4(a) and 4(b) present the pattern of the $z$ component of the electric field in the frequency domain for the resonant frequency $\omega=0.354$ at $\Delta r/a=0$ and 0.15, respectively.

Now, if the corner cell is distorted by the $B_2$ perturbation, the $|p_x+p_y\rangle$ and $|p_x-p_y\rangle$ states of the corner defect are split in energy by $\Delta\omega=2V_{xy}^{B2}$ (Fig. 2). The resonant transmission of the structure is observed when the $|p_x+p_y\rangle$ state of the corner defect has the same energy as the $|p_x\rangle$ band of the $x$ arm. We estimate that the maximum of the transmission will be observed when $\omega_{|px+py\rangle}\sim\omega_{\|}=0.354$. Taking the value $\omega_0=0.358$ for the undistorted $E$ defect state, we find from Fig. 2 that the maximum should be reached at $\Delta\omega\sim 0.008$. This value corresponds to the distortion of the lattice $\Delta r/a\sim 0.15$, in agreement with the FDTD calculations. We can follow in Fig. 3 how the split defect states shift with increasing the distortion, approaching the $p_{\|}$ and $p_{\perp}$ bands. The distribution of the $E_z$ field for $\Delta r/a=0$ and 0.15 presented in Fig. 4 gives an evidence that, in the case of $\Delta r=0$, light prefers to tunnel from the $p_x$ band of the

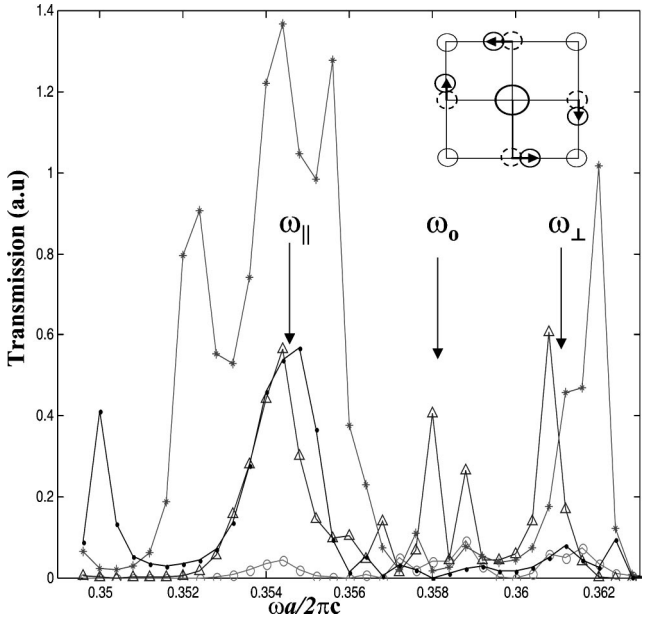


FIG. 3. The relative transmission intensity inside the band gap for the structures with $\Delta r/a=0$ (o markers), 0.05 (''up triangulars'' markers), 0.15 (star markers), and 0.3 (dot markers). The peaks corresponding to $p_{\|}$ and $p_{\perp}$ bands as well as for the defect $E$ states in the undistorted lattice are shown by arrows. Inset shows the corner cell distorted by means of the $B_2$ mode.

$x$ arm to the $p_x$ band of the $y$ arm [Fig. 4(a)], while for $\Delta r > 0$, the strongest coupling between the two branches manifests [Fig. 4(b)].

In conclusion, in this letter we have studied the transmission of the 90° bend coupled cavity waveguide based on two-dimensional photonic crystals. By exploiting the effect of symmetrical splitting of the doubly degenerate defect level, we have shown that the transmission of the structure can be tuned by the magnitude and symmetry of the lattice distortion. The effect is characterized by a resonant behavior, the maximum transmission corresponding to the frequencies of the waveguide branches that coincide with the frequency of the corner defect, providing the maximum coupling. The way to implement this device concept is to provide a local control of the distortion of the lattice or the defect rod by piezoelectric elements built directly beneath or above the waveguide corner.[11] One scheme would be to create a template for photonic rods by starting with a nonpiezoelectric substrate, and build piezoelectric patches using patterned thin films or crystal-ion slices that can be electrically controlled.[12] In the limit, each individual photonic rod can have its own actuator, which would then provide the ability to program arbitrary local motions of individual defect rods. For devices at 1.55 $\mu$m the piezoelectric elements should

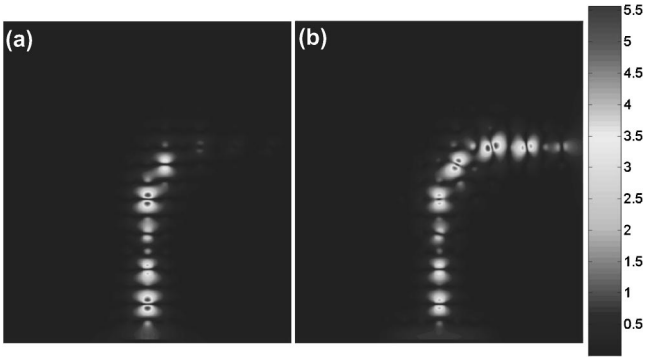


FIG. 4. Pattern of the $z$ component of the electric field in the frequency domain for the resonant frequency $\omega=0.354$ at $\Delta r/a=0$ (a) and 0.15 (b).

have a size of $\sim 3$ $\mu$m, while the rod displacements involved are $\sim 200$ nm, which are achievable with current piezoelectrics such as lead zinc niobate–lead titanate relaxor ferroelectrics. An easier approach might be to provide piezoelectric patches for a small cluster of rods or perhaps even the entire crystal. The last case, however, may result in undesirable changes to the lattice parameters, which can result in an overall scaling of photonic band frequencies. These changes, if small, will have to be modeled, and taken into account at the design level for such a device to operate.

The authors would like to acknowledge the support from the Center for Collective Phenomena in Restricted Geometries (Penn State MRSEC) under NSF Grant No. DMR-00800190, National Science Foundation Grant No. ECS-9988685, and the Center for Optical Technologies. The authors thank the Materials Simulation Center (Penn State) for the provision of the computer facilities.

[1] M. Bayidir, B. Temelkuran, and E. Ozbay, Phys. Rev. B **61**, R11855 (2000); M. Bayidir, S. Tanriseven, and E. Ozbay, Appl. Phys. A: Mater. Sci. Process. **72**, 117 (2001).
[2] A. Yariv, Y. Xu, R. K. Lee, and A. Scherer, Opt. Lett. **24**, 711 (1999).
[3] A. Mekis, J. C. Chen, I. Kurland, S. Fan, P. R. Villeneuve, and J. D. Joannopoulos, Phys. Rev. Lett. **77**, 3787 (1996).
[4] H. Takeda and K. Yoshino, Phys. Rev. B **67**, 073106 (2003).
[5] L. D. Landau and E. M. Liphshitz, *Quantum Mechanics* (Nauka, Moscow, 1974).
[6] K. Sakoda and H. Shiroma, Phys. Rev. B **56**, 4830 (1997).
[7] A. Taflove, S. C. Hagness, *Computational Electrodynamics: The Finite-Difference Time-Domain Method* (Artech House, Boston, 2000).
[8] A. Talneau, L. Le Gouezigou, N. Bouadma, M. Kafesaki, and C. M. Soukoulis, Appl. Phys. Lett. **80**, 547 (2002).
[9] I. B. Bersuker, *The Jahn–Teller Effect and Vibronic Interactions in Modern Chemistry* (Plenum, New York, 1983).
[10] R. D. Meade, K. D. Brommer, A. M. Rappe, and J. D. Joannopoulos, Phys. Rev. B **44**, 13772 (1991).
[11] S. Kim and V. Gopalan, Appl. Phys. Lett. **78**, 3015 (2001).
[12] R. M. Osgood, Jr., A. M. Radojevic, and M. Levy, AIP Conf. Proc. **576**, 896 (2001).